BIOCHEMISTRY
including biophysical chemistry & molecular biology

Article

pubs.acs.org/biochemistry

Investigating the Molecular Determinants for Substrate Channeling in BphI–BphJ, an Aldolase–Dehydrogenase Complex from the Polychlorinated Biphenyls Degradation Pathway

Jason Carere, Perrin Baker, and Stephen Y. K. Seah*

Department of Molecular and Cellular Biology, University of Guelph, Guelph, Ontario, Canada N1G 2W1

Supporting Information

ABSTRACT: BphI–BphJ, an aldolase–dehydrogenase complex from the polychlorinated biphenyls (PCBs) degradation pathway, cleaves 4-hydroxy-2-oxoacids to pyruvate and an aldehyde. The enzyme complex was shown to exhibit substrate channeling, whereby linear aldehydes of up to 6 carbons long and branched isobutyraldehyde were directly channeled from the aldolase to the dehydrogenase with greater than 80% efficiency. BphI variants G322F, G322L, and G323F were created and were found to block aldehyde channeling. The dehydrogenase cofactor NADH was able to activate the catalytic activity of the aldol cleavage reaction in these variants, suggesting that activation of BphI by BphJ cofactors is not solely due to faster aldehyde release. A G323L variant was able to channel acetaldehyde but not the larger propionaldehyde while the G323A variant was able to channel butyraldehyde but not its isomer isobutyraldehyde, confirming that the restricted channeling of aldehydes in these glycine variants are due to steric blockage of the channel. Substitution of His-20 and Tyr-290 in BphI led to significant reductions in aldehyde channeling efficiencies. A mechanism of substrate channeling involving these two gating residues is proposed.

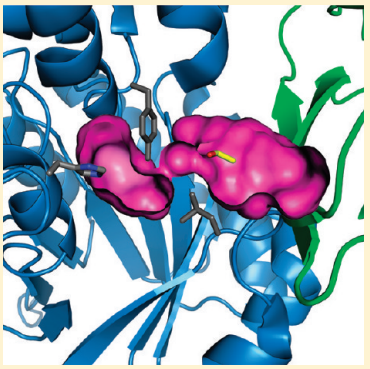

The microbial *meta*-cleavage pathway is important for the biodegradation of aromatic pollutants such as phenols, xylenes, and polychlorinated biphenyls (PCBs) and for host cholesterol utilization by the human pathogen, *Mycobacterium tuberculosis*.[1−3] These diverse aromatic compounds can be transformed in the pathway to form a 4-hydroxy-2-oxoacid intermediate. Carbon bond cleavage between the C3 and C4 of this intermediate by an aldolase leads to the formation of pyruvate and an aldehyde.[4] The latter is then converted to an acyl-CoA by an acylating acetaldehyde dehydrogenase. In the polychlorinated biphenyls degradation pathway of *Burkholderia xenovorans* LB400, the class II aldolase BphI forms a stable complex with the dehydrogenase, BphJ. Previously, using a substrate competition assay, it was demonstrated that acetaldehyde and propionaldehyde produced from the BphI-catalyzed cleavage of 4-hydroxy-2-oxopentanoate (HOPA) and 4-hydroxy-2-oxohexanoate (HOHA), respectively, are not released to the bulk solvent but are channeled directly to BphJ.[4] Thus, when excess propionaldehyde was added exogenously to a reaction mixture containing 4-hydroxy-2-oxopentanoate, 95% of the CoA esters produced were acetyl-CoA. Conversely, 99% of the CoA esters produced were propionyl-CoA when an excess of exogenous acetaldehyde was added in an enzyme reaction mixture containing 4-hydroxy-2-oxohexanoate. The K_m values for exogenous aldehydes in BphJ are >8 mM, and coupled to the fact that aldehydes are volatile, reactive, and toxic, channeling and sequestering of aldehydes from the cytoplasm of the bacterium may be necessary for efficient conversion to CoA esters and to prevent detrimental effects to the cell. Furthermore, it was observed that the k_{cat} value for BphI was increased about 4-fold when nicotinamide cofactors of the dehydrogenase were present, suggesting that communication between the enzymes in the complex ensured efficient coupling of their respective reactions.[4]

The crystal structure of orthologous aldolase–dehydrogenase complex (DmpG-DmpF; 56% and 55% sequence similarity to BphI and BphJ, respectively) from the phenol degradation pathway of *Pseudomonas putida* CF600 depicts a ∼21 Å long hydrophobic tunnel between the aldolase and the dehydrogenase active sites, providing a possible route for the direct diffusion of aldehyde from the aldolase to the dehydrogenase.[5] The presence of a conduit for the passage of common intermediates in sequential enzyme reactions has been observed in several other enzyme systems that exhibit substrate channeling, including tryptophan synthase, carbamoyl phosphate synthetase, and glucosamine 6-phosphate synthase.[6−8] Unique to the aldolase–dehydrogenase system of the aromatic degradation pathway is that the respective enzymes have broad substrate specificities and are capable of utilizing larger substrates.[9,10] While it has been demonstrated that acetaldehyde and propionaldehyde can be channeled by the enzyme complex, it was unclear if longer and branched aldehydes could also be channeled. This has some practical relevance since the *meta*-cleavage pathway for degradation of certain phenols with

Received: June 23, 2011
Revised: August 11, 2011
Published: August 12, 2011

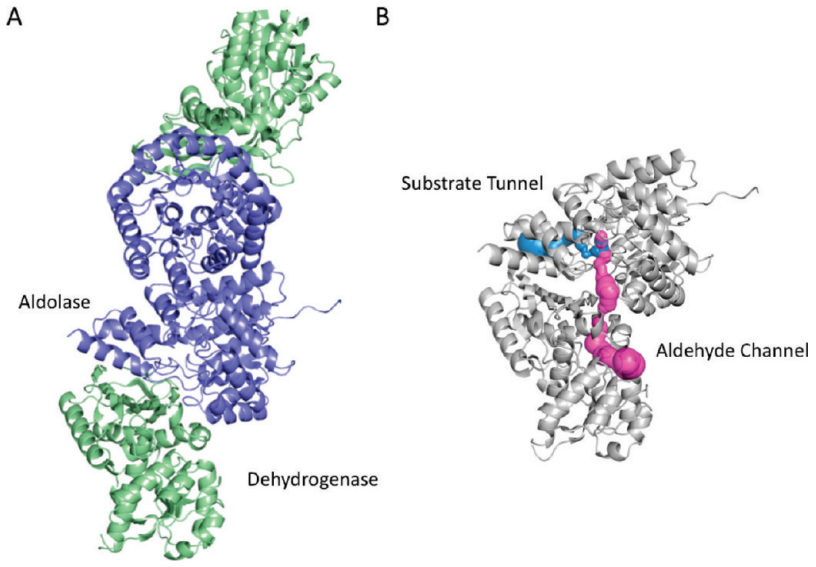

Figure 1. Structure of DmpG−DmpF showing (A) the tetrameric arrangement of the biological unit with aldolases colored blue and dehydrogenases colored green and (B) the location of the tunnel from the aldolase active site to the bulk solvent (blue) and the channel connecting the active sites of the aldolase to the dehydrogenase (magenta). The location of the tunnel and channel were determined using MOLE.[17] Images were generated using PyMOL.[18]

alkyl substitutions at the C4 position has been reported in bacteria, yielding aldehydes up to 7 carbon atoms in length.[11,12]

By a combination of molecular modeling and site-specific mutagenesis, we explored the contribution of residues in the enzyme complex that govern channeling specificity and efficiency. We developed a method to quantify the efficiency of aldehyde channeling in the BphI−BphJ complex which enabled us to determine channeling efficiencies of aldehydes of varying sizes and lengths. Finally, the creation of channel blocked enzyme variants enabled us to test if the observed 4-fold activation of BphI by BphJ when nicotinamide cofactor is bound is due to faster aldehyde release by substrate channeling.

MATERIALS AND METHODS

Chemicals. Sodium pyruvate, LDH (rabbit muscle), and all aldehydes were from Sigma-Aldrich (Oakville, ON). Restriction enzymes, T4 DNA ligase, and *Pfu Turbo* polymerase were from Stratagene (Mississauga, ON) or New England Biolabs (Pickering, ON). Ni-NTA Superflow resin was obtained from Qiagen (Mississauga, ON). 4-Hydroxy-2-oxoacids were synthesized using BphI or HpaI by previously described methods.[9] Aldehyde dehydrogenase from *Saccharomyces cerevisiae* was from Calzyme (San Luis Obispo, CA). All other chemicals were analytical grade and were obtained from either Sigma-Aldrich and Fisher Scientific (Nepean, ON).

Site-Directed Mutagenesis. DNA was purified using standard protocols.[13] *bph*I and *bph*J were previously cloned into the plasmids pBTL4-T7 and pET28a, respectively.[4] Site directed mutagenesis was performed using a Quickchange (Stratagene) method for I195L and I195F and a modified method[14] with nonoverlapping primers (Table S1) for other variants. Genes were sequenced at the Guelph Molecular Supercenter to confirm that the desired mutations were incorporated and the absence of secondary mutations. The L89A, H20A, and Y290F variants were created as previously reported.[10]

Structure Modeling and Sequence Alignment. A multiple-sequence alignment containing orthologous aldolases was generated using ClustalX[15] and visualized using ESPript.[16] Channels in the orthologous DmpG-DmpF complex from *P. putida* CF600 (PDB 1NVM)[5] were identified using MOLE[17] and visualized in PyMOL.[18]

Expression and Purification of the Enzyme Complex. Wild-type and variant BphI−BphJ enzyme complexes were expressed and purified as previously described.[4] Sodium dodecyl sulfate−polyacrylamide gel electrophoresis was performed and gels stained with Coomassie Blue to assess purity. Protein concentrations were assessed by Bradford Assay using bovine serum albumin as the standard.[19]

Steady-State Kinetic Assays. Aldolase cleavage activity was determined by coupling the production of pyruvate to NADH oxidation by LDH.[4] All assays were performed at least in duplicate, at 25 °C in a total volume of 1 mL using a Varian Cary 3 spectrophotometer with a thermojacketted cuvette holder. A standard assay contained 0.4 mM NADH, 1 mM $MnCl_2$, and 19.2 units LDH in 100 mM HEPES buffer (pH 8.0). The concentration of 4-hydroxy-2-oxoacids was varied from $0.1K_m$ to $5K_m$. Oxidation of NADH was monitored continuously at 340 nm with the extinction coefficient taken as 6200 M^{-1} cm^{-1}. To assess the activity of BphI and variants in the absence of BphJ cofactors, a discontinuous assay was utilized. Assay mixtures contain 1 mM $MnCl_2$, HOPA concentrations varied from $0.1K_m$ to $5K_m$, and 18 μg of BphI−BphJ in 100 mM HEPES buffer (pH 8.0). After 10 min, the reaction was quenched with 20 mM EDTA (pH 8.5) and 0.4 mM NADH. The amount of pyruvate produced was measured by an end-point assay with LDH.

The activity of the dehydrogenase, BphJ, was monitored continuously at 340 nm to observe the formation of NADH. Assays contained 0.4 mM NAD^+ and 0.1 mM coenzyme A in 100 mM HEPES buffer (pH 8.0) with varied aldehyde concentrations from $0.1K_m$ to $5K_m$. Kinetic parameters were determined as previously described, and results were fitted by nonlinear regression to the Michealis−Menten equation using Leonora.[4,20]

dx.doi.org/10.1021/bi200960j | *Biochemistry* 2011, 50, 8407−8416

Channeling Assays. The amount of aldehyde channeled directly from the aldolase to the dehydrogenase was assessed using an enzyme competition assay. All assays contained 0.4 mM NAD^+, 0.1 mM coenzyme A, 1 mM $MnCl_2$, 5 μg of enzyme (200 μg for the H20A and Y290F), and 20 U of aldehyde dehydrogenase (ALDH) in a total volume of 1 mL in 100 mM HEPES buffer pH 8.0. Reactions were initiated by addition of substrate, and the amount of NADH produced was measured spectrophotometrically at 340 nm. HOPA and HOHA concentrations were 25 μM for wild-type enzyme and G322, G323, and L89A variants while 200 μM was used for the less active variants, H20A and Y290F. Other 4-hydroxy-2-oxoacids concentrations were used at concentrations of 100 μM.The reaction was quenched after 5 min with 3 N HCl to a final concentration of 70 mM. The sample was centrifuged for 3 min at 21000*g* to pellet the denatured enzyme. A 500 μL sample of the reaction mixture was subjected to high performance liquid chromatography (HPLC) using an AKTA Explorer 100 (Amersham Pharmacia Biotech, Baie d'Urfe, QC) equipped with a HyPURITY C18 column (Thermo Scientific). Samples were eluted with 50 mM sodium phosphate (pH 5.3)−acetonitrile mixtures at the following ratios: 47:3 for acetyl-CoA and propionyl-CoA, 125:16 for butyryl-CoA and iso-butyrl-CoA, 25:4 for pentanoyl-CoA and hexanoyl-CoA. The flow rate was 1.0 mL/min, and CoA-esters were detected by UV absorbance at 254 nm. Quantification of the acyl-CoA molecules produced was completed using standard curves of the pure compounds. Pentanoyl-CoA standards are not commercially available and were synthesized using BphJ, pentaldehyde, CoA, and NAD^+. The channeling efficiency was calculated by comparing the acyl-CoA produced (determined using HPLC) to the concentration of 4-hydroxy-2-oxoacid utilized by BphI based on the amount of NADH produced by BphJ and ALDH (eq 1).

$$\text{channeling efficiency} = \frac{\text{Acyl-CoA produced}}{\text{total amount of aldehyde produced}} \times 100\% \quad (1)$$

RESULTS

Structural Analysis of the Channel Linking Active Sites of the Aldolase and Dehydrogenase. The crystal structure of the BphI−BphJ complex is not available; therefore, structural analysis was performed on the crystal structure of the orthologous enzymes, DmpG−DmpF, from *P. putida* CF600 (PDB 1NVM). The asymmetric unit in the crystal consists of two tetramers, with all aldolases (DmpG) containing bound Mn^{2+} and oxalate, a pyruvate enolate analogue, and three of the four dehydrogenase subunits (DmpF) containing bound NAD^+ (Figure 1A). The biological unit of the complex is a tetramer consisting of two DmpG subunits in the middle and each of the two DmpF subunits associating with each DmpG subunit at the periphery to form an elongated structure.[5] It has previously been determined by gel filtration that BphI−BphJ also forms a tetramer.[4] The position of the tunnel linking the bulk solvent to the active site and the channel linking the aldolase and dehydrogenase were mapped using the software MOLE using the crystal structure of DmpG−DmpF as template (Figure 1B).

A narrow tunnel connects the active site of the aldolase, DmpG, to the bulk solvent, which is presumably the entrance for 4-hydroxy-2-oxoacid substrates and the exit for the pyruvate product (Figure 2). The narrowest point of the tunnel connecting the active sites of DmpG−DmpF (1.6 Å in diameter) is insufficient in size to allow for passage of 4-hydroxy-2-oxoacids, and therefore rotation of the proposed catalytic base, His-21, is assumed to be required to allow for access of substrates.[5] Upon substrate entry, His-21 is proposed to revert back to its conformation seen in the "closed" position in order to be of optimal distance and geometry relative to the C4-OH of the substrate to be effective as a catalytic base.[10] Substrate binding is presumably also coordinated by a rotation about the Cα of Tyr-291 to relieve a steric clash between the hydroxyl oxygen of Tyr-291 and C4 of the modeled substrate.[10] Movement of Tyr-291 would result in an enlargement in the opening of the channel. Interestingly, when the aldehyde moiety of the 4-hydroxy-2-oxoacids is longer than 4 carbons in length, there is no space available in the active site to accommodate the longer alkyl chain unless the distal end of the molecule protrudes into the aldehyde channel (Figure 2).

The channel connecting the active sites of DmpG and DmpF is contributed almost entirely by the aldolase and residues that

Scheme 1. Cleavage of 4-Hydroxy-2-oxoacid to Pyruvate and an Aldehyde[a]

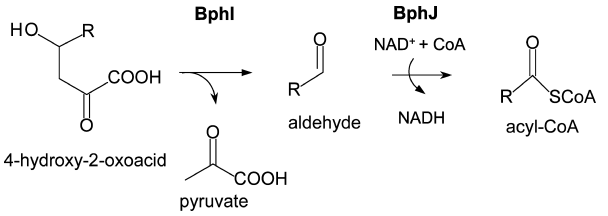

[a]The aldehyde is then channeled to BphJ where an acyl-CoA is produced using NAD^+ and CoA as cofactors. R = CH_3 in the biphenyl degradation pathway.

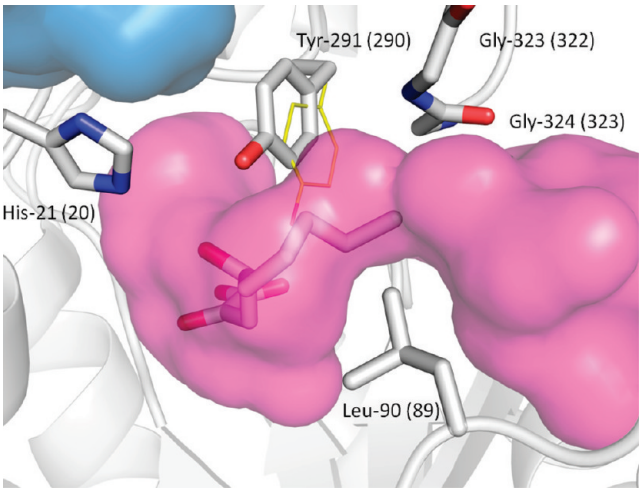

Figure 2. Model of 4-hydroxy-2-oxononanoate bound in the DmpG active site. The model was generated by superimposing the pyruvyl moiety of substrate shown in sticks within the active site on the experimentally observed oxalate. The tunnel leading from bulk solvent is shown in blue, and the active site and channel connecting the aldolase active site to the dehydrogenase is shown in magenta. His-21 blocks the tunnel leading from the bulk solvent. Residues investigated in this study are shown in sticks. Carbon atoms of Tyr-291 in the crystal structure is shown in yellow lines and the residue rotated 14° clockwise about the Cα to avoid steric slash with the C4 of the modeled substrate is shown in gray as sticks. Leu-90, Gly-323, and Gly-324 line the narrowest point of the tunnel. Corresponding residue numbers in BphI are indicated in brackets. The distal end of 4-hydroxy-2-nonanoate is too long to fit in the active site and is propose here to protrude into the channel.

dx.doi.org/10.1021/bi200960j | *Biochemistry* 2011, 50, 8407−8416

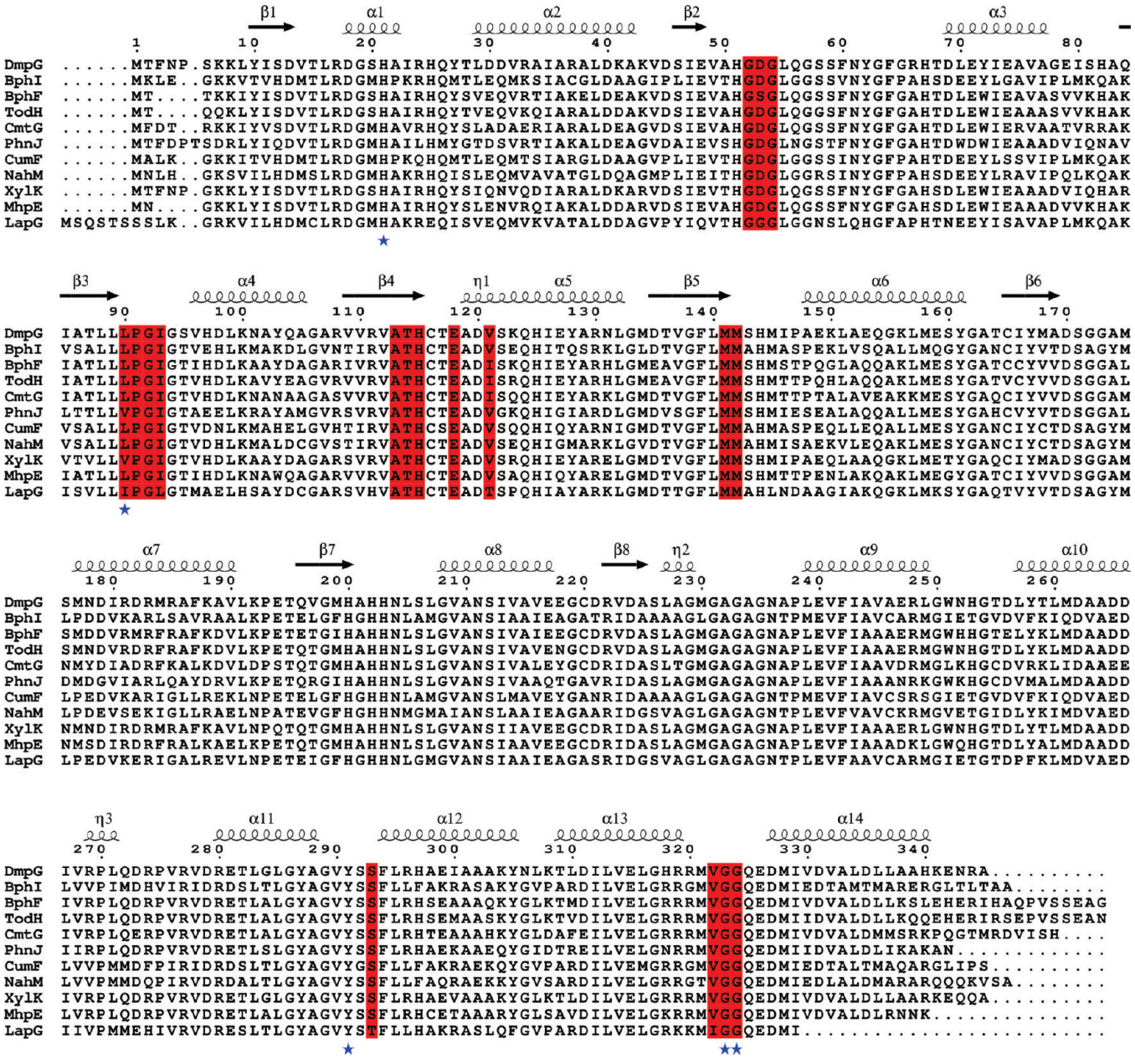

Figure 3. Sequence alignment of BphI and orthologes. Amino acid sequences of proteins and their uniprot accession number are as follows: DmpG from *Pseudomonas putida* CF600 (P51016), BphI from *B. xenovorans* (P51015), BphF from *Pseudomonas sp.* strain KKS102 (P51014), TodH from *Pseudomonas putida* F1 (P51018), CmtG from *Pseudomonas putida* F1 (Q51983), PhnJ from *Pseudomonas sp.* Strain DJ77 (Q9Z3U6), CumF from *Pseudomonas fluorescens* IP01 (P97092), NahM from *Pseudomonas putida* (P51017), XylK from *Pseudomonas putida* (P51019), MhpE from *Escherichia coli* (P51020), and LapG from *Pseudomonas alkylphenolia* (Q7WYE3). Secondary structures of DmpG are indicated as horizontal arrows (beta strands) and helices (α helix) above the sequences. Conserved residues that line the aldehyde channel are highlighted in red. Residues in BphI that were replaced by site-directed mutagenesis in this study are indicated by stars at the bottom of the alignment. This alignment was generated using ClustalX[15] and visualized using ESPript.[16]

compose the channel are conserved in orthologs, including BphI (Figure 3). The diameter of the aldehyde channel ranges between approximately 2.4 and 5.4 Å (Figure 4), with the narrowest point (diameter ~2.4 Å) lined by residues Gly-323 and Gly-324 on one side and the Cδ1 of Leu-90 on the opposite wall of the tunnel formed by the aldolase, DmpG. Together with the side chain of Tyr-291, the Cδ1 of Leu-90 creates the entrance of the aldehyde channel in the aldolase while the Cδ2 of Leu-90 forms one boundary of the active site of the aldolase (Figure 2). The exit of the channel, on the other hand, is formed by three residues of the dehydrogenase DmpF: Ile-172, Ile-196, and Met-198. These three residues adopt alternative conformations within and between the ligand free and ligand bound structures. In the absence of NAD^+, these residues block access to the active site of the dehydrogenase from the channel. However, in the NAD^+-bound form of the dehydrogenase, movement of the Ile-172 and Met-198 side chains results in a small opening of the exit of the channel (diameter ~1.7 Å).

To probe the contributions of specific residues in aldehyde channeling, several variants of the BphI−BphJ complex were created. Gly-322 and Gly-323 (Gly-323 and Gly-324 of DmpG)

dx.doi.org/10.1021/bi200960j | *Biochemistry* 2011, 50, 8407−8416

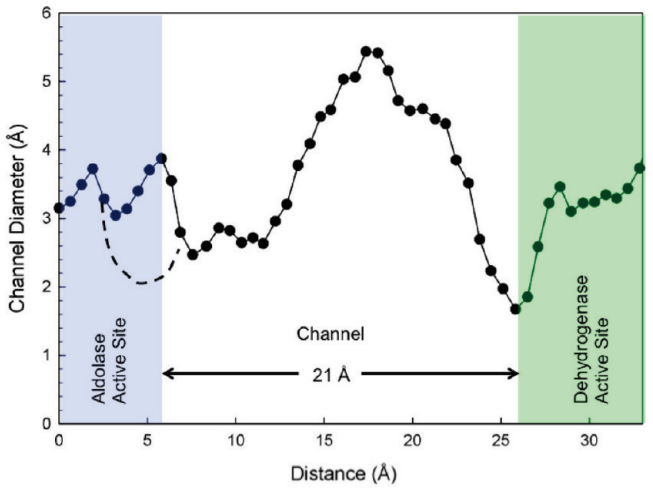

Figure 4. Graphical representation of the diameter of the aldehyde channel as determined using the program MOLE.[17] The tunnel was mapped from the position of the divalent metal cofactor in the aldolase to the putative catalytic cysteine in the dehydrogenase. Positions in the graph corresponding to the aldolase and dehydrogenase active sites are depicted in blue and green, respectively. Computation of the structure when Tyr-291 is in the "closed" conformation as in the crystal structure is shown as a dotted line. The "open" conformation as predicted by the model is a solid line. The first channel diameter minima at about 7 Å distance corresponds to the location of the two glycine residues (323 and 324 in DmpG) that line the channel.

were replaced with bulkier residues alanine, leucine, and phenylalanine. Leu-89 of BphI (Leu-90 in DmpG) was replaced with a smaller alanine residue. This set of variants was created to probe the effects of reducing or increasing the channel diameter on aldehyde channeling efficiencies. The contribution the proposed gating residues in aldehyde channeling was tested by replacement of His-20 of BphI (His-21 of DmpG) with alanine and Tyr-290 (Tyr-291 in DmpG) with phenylalanine. Ile-195 of BphJ (Ile-196 in DmpF) that forms the exit of the channel was replaced with an isosteric leucine residue and the larger phenylalanine residue.

Site-Specific Mutagenesis, Protein Purification, and Steady-State Kinetic Analysis. All variants were successfully created by site specific mutagenesis and purified using the same conditions as wild-type[4] enzyme with similar yields and purities achieved. Aldolase kinetic parameters of Y290F and H20A variants were previously reported,[10] and their catalytic efficiencies were lowered by ~3-fold and ~100-fold, respectively, relative to the wild-type aldolase. Steady-state kinetics of both the aldolase and dehydrogenase of other variants were determined and are of the same order of magnitude as the wild-type enzymes (Tables 1 and 2).

Determination of Aldehyde Channeling Efficiency in the Wild-Type BphI–BphJ Complex. Previously, using a substrate competition assay, it was demonstrated that the enzyme complex can channel acetaldehyde and propionaldehyde.[4] To obtain a quantitative measure of channeling efficiency, an enzyme competition assay was developed. Excess exogenous aldehyde dehydrogenase was added to the assay so aldehyde released to the bulk solvent would be oxidized to a carboxylic acid. In contrast, aldehydes channeled to BphJ will be converted to acyl CoA esters. The amount of acyl-CoA produced by the enzyme complex in relation to the total amount of aldehyde produced from the cleavage of 4-hydroxy-2-oxoacid by BphI provides a quantitative measure of efficiency of channeling for each aldehyde as indicated by eq 1. Channeling efficiency is defined here as the amount of aldehyde channeled from BphI which is utilized by BphJ to form CoA esters. It also depends on the degree of coupling between the reactions catalyzed by the aldolase and the dehydrogenase and represents a lower threshold for the true amount of aldehyde which traverses the channel.

Table 1. Steady-State Kinetic Constants of BphI and Variants for the Aldol Cleavage of HOPA and HOHA[a]

	substrate			
	HOPA		HOHA	
enzyme	K_m (μM)	k_{cat} (s^{-1})	K_m (μM)	k_{cat} (s^{-1})
WT	89 ± 8	4.07 ± 0.07	117 ± 10	3.9 ± 0.2
G322L	140 ± 10	1.09 ± 0.05	350 ± 20	0.94 ± 0.02
G323L	160 ± 20	0.64 ± 0.03	370 ± 70	0.27 ± 0.02
G322F	90 ± 10	1.06 ± 0.04	300 ± 20	1.05 ± 0.03
G323F	940 ± 80	4.3 ± 0.2	1100 ± 200	1.3 ± 0.1
G322A	180 ± 20	2.4 ± 0.1	520 ± 90	1.9 ± 0.1
G323A	60 ± 10	0.34 ± 0.02	360 ± 30	0.46 ± 0.07

[a]Aldolase assays were performed at 25 °C and contained 0.4 mM NADH, 1 mM $MnCl_2$, and 19.2 units LDH in 100 mM HEPES buffer (pH 8.0).

Table 2. Steady-State Kinetic Parameters of BphJ and Variants toward Acetaldehyde and Propionaldehyde[a]

	substrate			
	acetaldehyde		propionaldehyde	
enzyme	K_m (mM)	k_{cat} (s^{-1})	K_m (mM)	k_{cat} (s^{-1})
WT	24 ± 2	17.2 ± 0.5	23 ± 2	16.3 ± 0.5
I195F	35 ± 3	16 ± 1	48 ± 9	8.9 ± 0.8
I195L	7.4 ± 0.5	42 ± 2	7.7 ± 0.7	46 ± 2

[a]Dehydrogenase assays were performed at 25 °C and contained 0.4 mM NAD^+ and 0.1 mM coenzyme A in 100 mM HEPES buffer (pH 8.0).

Using this assay, channeling efficiency for acetaldehyde and propionaldehyde were determined to be 95 ± 5% and 95 ± 4%, respectively. Longer straight chain aldehydes up to six carbons in lengths were also tested and found to be efficiently channeled by the enzyme complex (Table 3). Surprisingly, the branched chain aldehyde, isobutyraldehyde, was also channeled with an efficiency similar to that of acetaldehyde, the physiological substrate of BphJ.

Role of Internal Channel Residues Gly-322, Gly-323, and Leu-89 in Aldehyde Channeling Efficiency and Specificity. Variants G322A and G323A were able to channel acetaldehyde with similar efficiencies to wild-type (Table 4). However, channeling efficiencies progressively decreased with increasing aldehyde chain length. The G322A variant was able to channel isobutyraldehyde, albeit at a 30% lower efficiency than the wild-type enzyme, but G323A variant was unable to channel this branched chain aldehyde. Channeling efficiency for acetaldehyde was lower in the G323L variant (63% efficiency), and this variant was unable to channel the larger propionaldehyde. The G322L, G322F, and G323F were all unable to channel either acetaldehyde or propionaldehyde. The kinetic parameters of the associated dehydrogenases in these variants were similar to the wild-type enzyme; thus, the reduced channeling efficiencies were not due to the compromised

dx.doi.org/10.1021/bi200960j | Biochemistry 2011, 50, 8407–8416

Table 3. Channeling Efficiencies of Various Aldehydes in Wild-Type BphI−BphJ Enzyme Complex[a]

	channeled aldehyde					
structure	acetaldehyde (CH_3CHO)	propionaldehyde (CH_3CH_2CHO)	butyraldehyde ($CH_3(CH_2)_2CHO$)	isobutyraldehyde ($(CH_3)_2CHCHO$)	pentaldehyde ($CH_3(CH_2)_3CHO$)	hexaldehyde ($CH_3(CH_2)_4CHO$)
channeling efficiency (%)	95 ± 5	95 ± 4	83 ± 2	92 ± 3	94 ± 4	84 ± 8

[a]Assays were performed at 25 °C and contained 0.4 mM NAD^+, 0.1 mM coenzyme A, 1 mM $MnCl_2$, and 5 μg BphI−BphJ in the presence of excess ALDH. Substrate concentration was 25 μM HOPA or HOHA and 100 μM for all other 4-hydroxy-2-oxoacids. CoA esters were detected at 254 nm by HPLC.

Table 4. Aldehyde Channeling Efficiencies of BphI Variants−BphJ Complexes

	channeling efficiency (%)					
BphI variant	acetaldehyde	propionaldehyde	butyraldehyde	isobutyraldehyde	pentaldehyde	hexaldehyde
G322A	89 ± 1	62 ± 7	74 ± 2	60 ± 3		
G323A	95 ± 10	58 ± 1	29 ± 3	0		
G322L	0	0				
G323L	62 ± 1	0				
G322F	0	0				
G323F	0	0				
L89A	67 ± 3	68 ± 1	79 ± 2	55 ± 2	67 ± 6	17 ± 1

activity of BphJ (Table S2). Creating a channel with a larger diameter by replacing Leu-89 located on the opposite side of Gly-322 and Gly-323 to alanine led to a surprising reduction in channeling efficiency of 30% for all aldehydes tested. The reduction of channeling efficiency in the variant could be due to the increased size of the channel entrance, subverting the gating mechanism, leading to escape of the aldehyde from the substrate entry/pyruvate exit tunnel.

Role of Ile-195, Tyr-290, and His-20 in Aldehyde Channeling. In contrast to the glycine variants, substitution of Ile-195 in BphJ to a bulkier phenylalanine residue did not significantly reduce the channeling efficiency of the enzyme complex toward acetaldehyde or propionaldehyde (Table 5).

Table 5. Channeling Efficiencies of Y290F and H20A Variants of BphI and I195 Variants in BphJ

	channeling efficiency (%)	
enzyme	acetaldehyde	propionaldehyde
I195L (BphJ)	79 ± 7	94 ± 1
I195F (BphJ)	80 ± 1	83 ± 5
Y290F (BphI)	57 ± 2	38 ± 1
H20A (BphI)	11 ± 3	15 ± 1

On the other hand, substitutions of the Tyr-290 in BphI with the smaller phenylalanine residue reduced channeling efficiencies by >30%. Replacement of His-20, a residue that gates the substrate entry tunnel, with alanine dramatically reduced acetaldehyde and propionaldehyde channeling by more than 70%.

Activation of Aldolase by Dehydrogenase in the Channeled Blocked Variant. On the basis of the crystal structure of the DmpG−DmpF complex, binding of nicotinamide induces the opening of the exit of the channel in the dehydrogenase, thus facilitating aldehyde channeling. We previously observed that BphI activity is activated 4-fold in the presence of NADH. To test if this activation is due to allosteric regulation of BphI by BphJ or simply faster product (aldehyde) release due to channeling, kinetic parameters for the glycine variants that block aldehyde channeling were determined (Table 6). The k_{cat} for the aldol cleavage of HOPA in the G322L, G322F, and G323F variants, which are unable to

Table 6. Steady-State Kinetic Constants of BphI and Glycine Variants for the Aldol Cleavage of HOPA in the Absence of BphJ Cofactors[a]

enzyme	K_m (μM)	k_{cat} (s^{-1})	fold activation of BphI by NADH[b]
WT	158 ± 20	0.79 ± 0.06	5.1 ± 0.4
G322L	81 ± 14	0.286 ± 0.02	3.8 ± 0.3
G323L	216 ± 7	0.100 ± 0.009	6.4 ± 0.6
G322F	53 ± 13	0.45 ± 0.07	2.4 ± 0.2
G323F	130 ± 10	0.72 ± 0.02	6.0 ± 0.2

[a]Assays contained 1 mM $MnCl_2$, HOPA concentrations varied from $0.1K_m$ to $5K_m$ in 100 mM HEPES buffer (pH 8.0). [b]Ratio of k_{cat} of BphI in the presence of NADH to the k_{cat} in the absence of NADH. BphI variants are in complex with wild-type BphJ.

channel aldehyde, were still higher by about 3−6-fold in the presence of NADH. This indicates that faster aldehyde release in the aldolase due to aldehyde channeling is not solely responsible for the activation of BphI by BphJ.

DISCUSSION

Substrate channeling involves the transfer of a common intermediate from one enzyme to another without release into bulk solvent.[21] In the case of the aldolase−dehydrogenase complex in aromatic degradation pathways, sequestering of volatile aldehydes from cellular components is beneficial because it prevents toxicity associated with reactive aldehydes and overcomes the inefficiency of the dehydrogenase for processing exogenous aldehydes due to high K_m values.

Probing the Route and Diameter of the Channel. Analysis of the DmpG−DmpF crystal structure showed that residues forming the channel that link the active sites of the aldolase and dehydrogenase are predominantly provided by the aldolase and are highly conserved in orthologous complexes. The molecular dimensions of the channel in the aldolase−dehydrogenase complex, with a narrowest diameter of 2.4 Å, appear to be incompatible for passage for the channeled

aldehyde (4.3 Å). This suggests that the channel is not rigid but dynamic movement of residues lining the channel is required to allow the intermediate to pass through. While the low *B*-factors of the channel in the crystal structure of DmpG−DmpF can indicate rigidity, this may be due to crystal packing constraints. Alternatively, since the structure does not contain aldehyde in the channel, it does not represent the complex during substrate channeling. Protein dynamics have also been suggested to occur in other enzyme systems that exhibit substrate channeling, including glutamine-dependent NAD^+ synthetase[22] and proline utilization A flavoenzyme (PutA).[23] In each case constrictions were observed in the structure of the channel, and therefore significant movement of residues in the channels is required to enable the passage of the channeled intermediate.

It has been determined previously that BphI and BphJ have broad substrate specificity,[4,10] although preceding enzymes in the PCBs degradation pathway have not been shown to utilize substrates that will lead to formation of compounds larger than 4-hydroxy-2-oxohexanoate. It is therefore surprising that aldehydes up to 6 carbons in length are channeled from the aldolase to the dehydrogenase with comparable channeling efficiency to that of acetaldehyde. The fact that the branched chain isobutyraldehyde can also be channeled by the complex indicates that these straight-chain aldehydes need not necessarily adopt an extended conformation in order to transverse from the aldolase to the dehydrogenase. Flexibility of the tunnel of carbamoyl phosphate synthetase has also been suggested to account for the ability for the enzyme to channel the larger hydrazine and hydroxylamine in addition to its natural channeled substrate, ammonia,[24] although the efficiency of channeling of these larger amines relative to ammonia has not been quantified.

Evidence that the putative tunnel identified from the crystal structure is indeed the route taken by channeled aldehydes was supported by the results from replacements of two residues, Gly-322 and Gly-323, which line the narrowest diameter of the channel. The G322L and G322F variants completely abrogate substrate channeling, suggesting that these residues have effectively blocked the channel while the G322A variant displayed ∼20% reduced aldehyde channeling efficiencies relative to the wild-type complex. On the other hand, as the side-chain size at position 323 was increased, the size of the aldehyde that these variants could efficiently channel became progressively smaller, supporting the premise that lower channeling efficiencies observed in the variants are due to steric blockage of the channel. In tryptophan synthase, physical blockage of indole channeling has also been attempted by replacing a cysteine residue (Cys-170) with tryptophan and phenylalanine, resulting in reduced indole channeling rate by at least 10- and 5000-fold, respectively.[25] In carbamoyl phosphate synthetase, replacement of Gly-359 with phenylalanine or tyrosine residues blocked ammonia channeling, manifested by uncoupling of hydrolysis of glutamine to carbamoyl phosphate formation and a lag in the time course for carbamoyl phosphate formation.[24] A G359S variant in carbamoyl phosphate synthetase exhibited reduced ammonia channeling while preventing hydroxylamine channeling while the G359L variant is defective in channeling both compounds.

Channel Entrance and Exit Residues. Previous steady-state kinetic analysis of BphI indicated that the enzyme follows an ordered sequential mechanism whereby the acetaldehyde product must leave the active site first prior to the release of the other product, pyruvate.[9] Intuitively this is important to allow the channeling of the aldehyde prior to the release of pyruvate. A reduction in aldehyde channeling efficiency was observed when two residues His-20 and Tyr-290, present at the substrate entrance and aldehyde channel entrance, were replaced by alanine and phenylalanine, respectively. It appears that these residues may be imperative in ensuring the coordinated release of products and preventing escape of acetaldehyde from the substrate entrance/pyruvate release site in BphI. When His-20, the proposed catalytic base of the enzyme, is poised for C4-OH proton abstraction of the substrate, the substrate entry/pyruvate release tunnel that leads from the aldolase active site to the bulk solvent is closed. This presumably prevents aldehyde from escaping through this route following C−C bond cleavage of the substrate. The H20A variant is still active, albeit with a 45-fold lowering of k_{cat}, due to hydroxide ions replacing the function of the catalytic base in the variant.[10] The variant however displayed a marked reduction (>70% reduction) in aldehyde channeling efficiency, possibly due to the fact that the methyl side chain of alanine is insufficient in size to effectively block the escape of aldehydes from the aldolase. In the proline dehydrogenase, PutA, which channels a pyrroline-5-carboxylate intermediate, a tyrosyl residue (Tyr-437) has been similarly observed to block the active site of the dehydrogenase domain from the bulk solvent.[26] This residue could potentially function as a substrate entry gate analogous to that of His-20 in BphI.

We previously demonstrated that the invariant tyrosine residue in the active site of BphI is not the catalytic acid, contrary to a previously proposed mechanism which suggested that during proton transfer torsional movement of Tyr-290 results in an opening of the channel entrance allowing for aldehyde channeling to the dehydrogenase to occur.[10] Closer inspection of the active site of the aldolase suggests that the binding of the modeled 4-hydroxy-2-oxoacid substrate will result in a steric clash between the C4 of the substrate and the oxygen in the *para* position of the phenol ring, necessitating the movement of this residue upon substrate binding which could lead to the opening of the tunnel for aldehyde channeling prior to the aldol cleavage reaction.[10] Upon cleavage of the 4-hydroxy-2-oxoacid, the aldehyde is released into the tunnel and Tyr-290 may adopt a closed conformation, as visualized in the crystal structure of DmpG−DmpF, preventing the back-diffusion of the aldehyde. In the BphI Y290F variant, channeling efficiency was reduced by about 30%, and this could be due either to relief of the steric constraint that is required for tunnel entrance opening or to the fact that the tunnel cannot be closed completely, allowing some aldehydes to escape from the aldolase through the substrate entry/pyruvate release site. Aromatic residues have been proposed as gating residues in other enzyme systems that exhibits substrate channeling. For example, the indole side chain of Trp-74 was observed to adopt an alternative rotameric conformation that opens the ammonia tunnel when a glutamine analogue was bound in the enzyme.[27] In tryptophan synthase movement of Phe-280 in the presence of K^+ and Cs^+ results in opening of the indole channel.[28]

When Leu-89 in BphI was replaced with the smaller alanine residue, aldehyde channeling efficiencies were also reduced. The delta carbons of Leu-89 form two faces of the tunnel. Cδ1 is directly opposite to Gly-322 and Gly-323 while Cδ2 forms the base of the active side of the aldolase. Replacing Leu-89 with alanine increases the size of the active site of the aldolase and should broaden the aldehyde channel. Enlargement of the

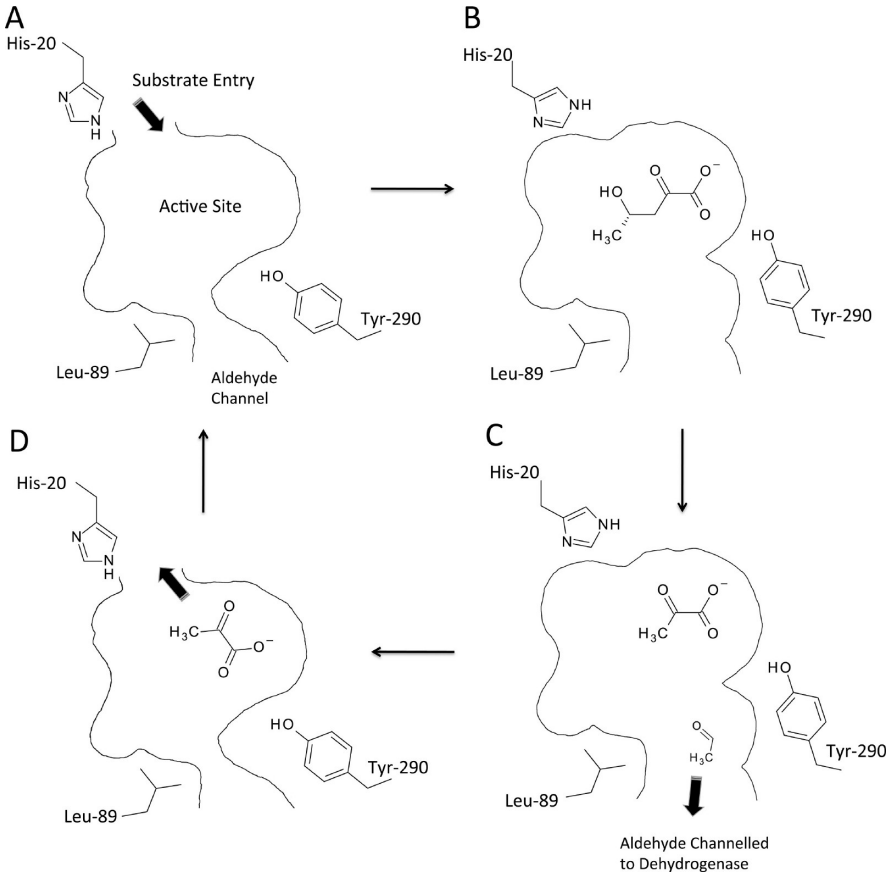

Figure 5. Proposed mechanism of substrate channeling in BphI–BphJ. (A) 4-Hydroxy-2-oxopentanoate (HOPA) enters the aldolase through the substrate tunnel where it passes His-20. (B) Upon substrate entry, Tyr-290 rotates to accommodate the substrate in the active site, thus opening the aldehyde channel. His-20 adopts a closed conformation and abstracts a proton from the C4-OH of the substrate to initiate the aldol cleavage reaction. (C) Upon aldol cleavage, the acetaldehyde is channeled to the dehydrogenase via the aldehyde channel and Tyr-290 reverts to a "closed" position, preventing the aldehyde from diffusing back into the aldolase active site. (D) His-20 adopts an "open" conformation, allowing pyruvate to leave and a second molecule of substrate to enter.

aldolase active site in the L89A variant has been demonstrated to increase the specificities of the aldolase for butyraldehyde, pentaldehyde, and hexaldehyde while maintaining similar specificities for acetaldehyde and propionaldehyde.[10] However, this modification had negative effects for aldehyde channeling, suggesting that the channel cannot be closed since the entrance to the tunnel is now widened (Figure S1).

In contrast to the significant effects in aldehyde channeling when the residues at the entrance of the aldehyde tunnel are replaced, replacement of Ile-195 at the exit of the tunnel in BphJ with a larger phenylalanine did not reduce aldehyde channeling. This implies that significant conformation changes on the channel exit residues can occur to allow for aldehydes to enter the dehydrogenase active site from the channel.

Activation of Aldolase Activity by the Dehydrogenase. The asymmetric unit in the crystal of DmpG–DmpF consists of two tetramers, with three of the four DmpF subunits containing bound NAD^+. In the crystal structure of DmpG–DmpF, three residues at the exit of the dehydrogenase adopt different conformations and only in the NAD^+ bound form was the channel exit opened for aldehyde to enter the dehydrogenase active site. It has been determined that NADH activates the aldolase reaction by 4-fold in the BphI–BphJ complex.[4] The BphI G322L, G323L, and G323F variants which completely lack the ability to channel acetaldehyde were found to be activated similar to the wild-type in the presence of NADH. The activation of BphI by BphJ is due to allosteric communication between the two enzymes rather than faster aldehyde release through the channel.

Proposed Mechanism of Substrate Channeling. Based on the results presented above, combined with previous work on the catalytic mechanism of the aldolase,[10] a mechanism for aldehyde channeling in the aldolase–dehydrogenase complex is proposed (Figure 5). In this mechanism the 4-hydroxy-2-oxoacid enters the aldolase through the substrate tunnel where it encounters His-20, which undergoes a conformation change to allow the 4-hydroxy-2-oxoacid to enter the active site of the aldolase. Following substrate entry, Tyr-290 rotates to accommodate the substrate in the active site, thus opening the aldehyde channel. The distal end of the alkyl side chains of aldehydes >4C in length protrude into the channel. His-20 adopts a "closed" conformation which also enables it to abstract a proton from C4-OH to initiate aldol cleavage. The aldehyde is released into the channel allowing for the torsional movement of Tyr 290 to a "closed" position, preventing the aldehyde from diffusing back into the aldolase active site. His-20 opens the substrate entry tunnel, allowing pyruvate to leave and a second molecule of substrate to enter.

■ CONCLUSION

Analysis of the crystal structure of the aldolase–dehydrogenase complex enabled the identification of a possible route for the

dx.doi.org/10.1021/bi200960j | *Biochemistry* 2011, 50, 8407–8416

direct channeling of aldehyde products from the aldolase to the dehydrogenase. The channel appears to be dynamic, and therefore the dimensions of the channel derived from the static crystal structure are inadequate in predicting the sizes of aldehydes that can diffuse through the channel. The coordinated conformational changes of specific gating residues appears to ensure the efficient channeling of aldehydes. The results presented here complement our previous biochemical data[4,9,10] and provide a structural basis for understanding how substrate channeling occurs in this enzyme complex.

■ ASSOCIATED CONTENT

Supporting Information

Primers used in PCR site-directed mutagenesis (Table S1); kinetic constants of the dehydrogenase associated with the BphI glycine variants (Table S2); model of the L89A variant (Figure S1). This material is available free of charge via the Internet at http://pubs.acs.org.

■ AUTHOR INFORMATION

Corresponding Author

*E-mail: sseah@uoguelph.ca. Phone: (519) 824 4120 Ext 56750. Fax: (519) 837 1802.

Funding

This research is supported by National Science and Engineering Research Council of Canada (NSERC), Grant 238284, to S.Y.K.S. P.B. is a recipient of a NSERC PGS-D scholarship.

■ ABBREVIATIONS

ADH, alcohol dehydrogenase; ALDH, aldehyde dehydrogenase; HEPES, 4-(2-hydroxyethyl)-1-piperazinepropanesulfonic acid; HOHA, 4-hydroxy-2-oxohexanoate; HOPA, 4-hydroxy-2-oxopentanoate; IPTG, isopropyl β-D-thiogalactopyranoside; LDH, L-lactate dehydrogenase.

■ REFERENCES

(1) Vander Geize, R., Yam, K., Heuser, T., Wilbrink, M. H., Hara, H., Anderton, M. C., Sim, E., Dijkhuizen, L., Davies, J. E., Mohn, W. W., and Eltis, L. D. (2007) A gene cluster encoding cholesterol catabolism in a soil actinomycete provides insight into Mycobacterium tuberculosis survival in macrophages. *Proc. Natl. Acad. Sci. U. S. A. 104*, 1947−1952.

(2) Furukawa, K., and Kimura, N. (1995) Biochemistry and genetics of PCB metabolism. *Environ. Health Perspect. 103* (Suppl. 5), 21−23.

(3) Furukawa, K., Hirose, J., Suyama, A., Zaiki, T., and Hayashida, S. (1993) Gene components responsible for discrete substrate specificity in the metabolism of biphenyl (bph operon) and toluene (tod operon). *J. Bacteriol. 175*, 5224−5232.

(4) Baker, P., Pan, D., Carere, J., Rossi, A., Wang, W., and Seah, S. Y. (2009) Characterization of an aldolase-dehydrogenase complex that exhibits substrate channeling in the polychlorinated biphenyls degradation pathway. *Biochemistry 48*, 6551−6558.

(5) Manjasetty, B. A., Powlowski, J., and Vrielink, A. (2003) Crystal structure of a bifunctional aldolase-dehydrogenase: sequestering a reactive and volatile intermediate. *Proc. Natl. Acad. Sci. U. S. A. 100*, 6992−6997.

(6) Hyde, C. C., Ahmed, S. A., Padlan, E. A., Miles, E. W., and Davies, D. R. (1988) Three-dimensional structure of the tryptophan synthase alpha 2 beta 2 multienzyme complex from Salmonella typhimurium. *J. Biol. Chem. 263*, 17857−17871.

(7) Thoden, J. B., Holden, H. M., Wesenberg, G., Raushel, F. M., and Rayment, I. (1997) Structure of carbamoyl phosphate synthetase: a journey of 96 A from substrate to product. *Biochemistry 36*, 6305−6316.

(8) Teplyakov, A., Obmolova, G., Badet, B., and Badet-Denisot, M. A. (2001) Channeling of ammonia in glucosamine-6-phosphate synthase. *J. Mol. Biol. 313*, 1093−1102.

(9) Wang, W., Baker, P., and Seah, S. Y. (2010) Comparison of two metal-dependent pyruvate aldolases related by convergent evolution: substrate specificity, kinetic mechanism, and substrate channeling. *Biochemistry 49*, 3774−3782.

(10) Baker, P., Carere, J., and Seah, S. Y. (2011) Probing the Molecular Basis of Substrate Specificity, Stereospecificity, and Catalysis in the Class II Pyruvate Aldolase, BphI. *Biochemistry 50*, 3559−3569.

(11) Cho, J. H., Jung, D. K., Lee, K., and Rhee, S. (2009) Crystal structure and functional analysis of the extradiol dioxygenase LapB from a long-chain alkylphenol degradation pathway in Pseudomonas. *J. Biol. Chem. 284*, 34321−34330.

(12) Jeong, J. J., Kim, J. H., Kim, C. K., Hwang, I., and Lee, K. (2003) 3- and 4-alkylphenol degradation pathway in Pseudomonas sp. strain KL28: genetic organization of the lap gene cluster and substrate specificities of phenol hydroxylase and catechol 2,3-dioxygenase. *Microbiology 149*, 3265−3277.

(13) Sambrook, J., Fritsch, E. F., and Maniatis, T. (1989) *Molecular Cloning: A Laboratory Manual*, Cold Spring Harbor Laboratory Press, Plainview, NY.

(14) Liu, H., and Naismith, J. H. (2008) An efficient one-step site-directed deletion, insertion, single and multiple-site plasmid mutagenesis protocol. *BMC Biotechnol. 8*, 91.

(15) Larkin, M.A., Blackshields, G., Brown, N. P., Chenna, R., McGettigan, P. A., McWilliam, H., Valentin, F., Wallace, I. M., Wilm, A., Lopez, R., Thompson, J. D., Gibson, T. J., and Higgins, D. G. (2007) Clustal W and Clustal X version 2.0. *Bioinformatics 23*, 2947−2948.

(16) Gouet, P., Courcelle, E., Stuart, D. I., and Metoz, F. (1999) ESPript: analysis of multiple sequence alignments in PostScript. *Bioinformatics 15*, 305−308.

(17) Petrek, M., Kosinova, P., Koca, J., and Otyepka, M. (2007) MOLE: a Voronoi diagram-based explorer of molecular channels, pores, and tunnels. *Structure 15*, 1357−1363.

(18) Delano, W. L. (2002) *The PyMOL Molecular Graphics System*, DeLano Scientific, San Carlos, CA.

(19) Bradford, M. M. (1976) A rapid and sensitive method for the quantitation of microgram quantities of protein utilizing the principle of protein-dye binding. *Anal. Biochem. 72*, 248−254.

(20) Cornish-Bowden, A. (1995) *Analysis of Enzyme Kinetic Data*, Oxford Univeristy Press, New York.

(21) Spivey, H. O., and Ovadi, J. (1999) Substrate channeling. *Methods 19*, 306−321.

(22) LaRonde-LeBlanc, N., Resto, M., and Gerratana, B. (2009) Regulation of active site coupling in glutamine-dependent NAD(+) synthetase. *Nat. Struct. Mol. Biol. 16*, 421−429.

(23) Srivastava, D., Schuermann, J. P., White, T. A., Krishnan, N., Sanyal, N., Hura, G. L., Tan, A., Henzl, M. T., Becker, D. F., and Tanner, J. J. (2010) Crystal structure of the bifunctional proline utilization A flavoenzyme from Bradyrhizobium japonicum. *Proc. Natl. Acad. Sci. U. S. A. 107*, 2878−2883.

(24) Huang, X., and Raushel, F. M. (2000) Restricted passage of reaction intermediates through the ammonia tunnel of carbamoyl phosphate synthetase. *J. Biol. Chem. 275*, 26233−26240.

(25) Schlichting, I., Yang, X. J., Miles, E. W., Kim, A. Y., and Anderson, K. S. (1994) Structural and kinetic analysis of a channel-impaired mutant of tryptophan synthase. *J. Biol. Chem. 269*, 26591−26593.

(26) Zhang, M., White, T. A., Schuermann, J. P., Baban, B. A., Becker, D. F., and Tanner, J. J. (2004) Structures of the Escherichia coli PutA proline dehydrogenase domain in complex with competitive inhibitors. *Biochemistry 43*, 12539−12548.

(27) Mouilleron, S., Badet-Denisot, M. A., and Golinelli-Pimpaneau, B. (2006) Glutamine binding opens the ammonia channel and activates glucosamine-6P synthase. *J. Biol. Chem. 281*, 4404−4412.

(28) Rhee, S., Parris, K. D., Ahmed, S. A., Miles, E. W., and Davies, D. R. (1996) Exchange of K+ or Cs+ for Na+ induces local and long-

range changes in the three-dimensional structure of the tryptophan synthase alpha2beta2 complex. *Biochemistry 35*, 4211−4221.